Oxidative Stress and Cytotoxicity Induced by Ferric-Nitrilotriacetate in HepG2 Cells That Express Cytochrome P450 2E1

KOICHI SAKURAI and ARTHUR I. CEDERBAUM

Department of Biochemistry, Mount Sinai School of Medicine, New York, New York 10029

This paper is available online at http://www.molpharm.org

ABSTRACT

Iron can potentiate the toxicity of ethanol. Ethanol increases the content of cytochrome P450 2E1 (CYP2E1), which generates reactive oxygen species, and transition metals such as iron are powerful catalysts of hydroxyl radical formation and lipid peroxidation. Experiments were carried out to attempt to link CYP2E1, iron, and oxidative stress as a potential mechanism by which iron increases ethanol toxicity. The addition of ferric-nitrilotriacetate (Fe-NTA) to a HepG2 cell line expressing CYP2E1 decreased cell viability, whereas little effect was observed in control cells not expressing CYP2E1. Toxicity in the CYP2E1-expressing cells was markedly enhanced after the depletion of glutathione. Lipid peroxidation was increased by Fe-NTA, especially in cell extracts and medium from the CYP2E1-expressing cells. Toxicity was completely prevented by vitamin E or by 6-hydroxy-2,5,7,8-tetramethylchroman-2-carboxylic acid, which also decreased the lipid peroxidation.

Levels of ATP were lowered by Fe-NTA, and this was associated with a decreased rate of oxygen consumption by permeabilized cells with substrates donating electrons to complexes I, II, and IV of the respiratory chain. This mitochondrial damage was prevented by vitamin E. Toxicity was accompanied by DNA fragmentation, and this fragmentation was prevented by antioxidants. Overexpression of bcl-2 decreased the toxicity and DNA fragmentation produced by the combination of CYP2E1 plus Fe-NTA, as did a peptide inhibitor of caspase 3. These results suggest that elevated generation of reactive oxygen species in HepG2 cells expressing CYP2E1 leads to lipid peroxidation in the presence of iron, and the ensuing prooxidative state damages mitochondria, releasing factors that activate caspase 3, leading to a loss in cell viability and DNA fragmentation.

The toxicity produced by iron in biological systems generally is ascribed to the enhanced production of powerful oxidants capable of initiating and propagating lipid peroxidation processes, oxidizing proteins, and damaging DNA (Halliwell and Gutteridge, 1984). One suggested mechanism by which ethanol can damage the liver involves the formation of reactive oxygen intermediates, lipid peroxidation, and oxidative stress (Nordmann *et al.*, 1992). This has led to an interest in the effects of ethanol on iron homeostasis. Acute and chronic ethanol treatment of rodents has been shown to elevate the nonheme iron content of the liver (Rouach *et al.*, 1990; Sadrrzadeh *et al.*, 1994; Tsukamoto *et al.*, 1995; Valerio *et al.*, 1996). An increased level of nonheme iron was observed in mitochondrial, cytosolic, and microsomal fractions of rat liver after acute ethanol treatment, with maximal increases in the microsomal fraction (Rouach *et al.*, 1990). Uptake of iron by isolated rat hepatocytes was enhanced after chronic ethanol feeding (Zhang *et al.*, 1993). Acute administration of ethanol plus iron resulted in extensive lipid peroxidation of rat liver (Valenzuela *et al.*, 1983). The addition of carbonyl iron to a liquid diet exacerbated the chronic ethanol-induced accumulation of fat and hydroxyproline while potentiating the decline in GSH levels, and it was concluded that the combination of ethanol plus iron potentiated lipid peroxidation and initiated prefibrotic events (Valerio *et al.*, 1996). In the intragastric infusion model of alcoholic liver disease, the addition of carbonyl iron resulted in further elevations of MDA and HNE, in transaminase levels, and in liver fibrosis, leading to the conclusion of there being a critical role for iron and iron-catalyzed oxidative stress in the progression of alcoholic liver disease (Tsukamoto *et al.*, 1995). Indeed, the

---

ABBREVIATIONS: GSH, glutathione, reduced form; BSO, buthionine sulfoximine; DMSO, dimethylsulfoxide; E9, HepG2-MV2E1–9 cells expressing CYP2E1; FBS, fetal bovine serum; HEPES, 4-(2-hydroxyethyl)-1-piperazineethanesulfonic acid; HNE, 4-hydroxyl-2-nonenal; LDH, lactate dehydrogenase; MDA, malonaldehyde; MEM, minimum essential medium; MTT, 3-[4,5-dimethylthiazol-2-yl]-2,5-diphenyltetrazolium bromide; MV5, HepG2-MV5 cells infected with virus lacking the CYP2E1 cDNA insert; NTA, nitrilotriacetic acid; PBS, phosphate-buffered saline; SOD, superoxide dismutase; TE, Tris/EDTA; TUNEL, terminal deoxynucleotidyl transferase-mediated dUTP-biotin nick end-labeling.

addition of an oral iron chelator decreased hepatic free iron concentration, lipid peroxidation, and fat accumulation in rats chronically consuming ethanol (Sadrrzadeh *et al.*, 1994). The addition of iron chelates to isolated microsomes from chronic ethanol-fed rats resulted in increased lipid peroxidation and hydroxyl radical formation compared with results with control microsomes (Cederbaum, 1989; Castillo *et al.*, 1992).

Although the above studies seem to indicate that iron can increase the toxicity of ethanol, the exact mechanism for this potentiation is not clear. Ethanol can increase the content of CYP2E1, a cytochrome P450 that is very reactive in oxidizing ethanol to acetaldehyde and in oxidizing many agents to reactive metabolites that are hepatotoxic (Lieber, 1997). CYP2E1 is very reactive in oxidizing NADPH and in the production of O_2^- and H_2O_2 during microsomal mixed-function oxidase activity (Gorsky *et al.*, 1984; Ekstrom and Ingelman-Sundberg, 1989). Induction of CYP2E1 and formation of reactive intermediates may be an important pathway by which ethanol produces oxidative stress. Correlations among induction of CYP2E1, lipid peroxidation, and ethanol-induced liver injury have been found in the intragastric infusion model of ethanol-induced liver injury (Castillo *et al.*, 1992; Morimoto *et al.*, 1994; Sadrrzadeh *et al.*, 1994; Tsukamoto *et al.*, 1995).

The goal of the current report was to evaluate the ability of iron to promote toxicity by a CYP2E1-dependent pathway. A HepG2 cell line established by retroviral infection to constitutively express human CYP2E1 (Dai *et al.*, 1993) was used in these experiments. The iron chelate used was Fe-NTA because this iron complex has been shown to produce hepatic lesions related to parenchymal cell iron disposition (Parmley *et al.*, 1981), is rapidly taken up by cells in culture (Sturrock *et al.*, 1990), and is a potent inducer of lipid peroxidation (Goddard and Sweeney, 1983). Free radicals have been shown to play a critical role in tissue damage induced by Fe-NTA (Fukuda *et al.*, 1996). The effect of Fe-NTA on viability, DNA fragmentation and lipid peroxidation of control HepG2 cells and HepG2 cells expressing CYP2E1, and modulation of these effects by antioxidants, bcl-2, and an inhibitor of caspase 3 was the focus of these studies.

Materials and Methods

Chemicals. FBS, MEM, antibiotics, and G418 were obtained from Life Technologies (Gaithersburg, MD). Ferric nitrate, NTA, vitamin E phosphate, BSO, malic acid, succinic acid, pyruvic acid, and ATP Assay Kit were from Sigma Chemical (St. Louis, MO). Succinic acid and pyruvic acid were neutralized by titration with 1 N KOH. Trolox (6-hydroxy-2,5,7,8-tetramethyl chroman-2-carboxylic acid) and digitonin were from Aldrich (Milwaukee, WI). The MTT Assay Kit was from Promega (Madison, WI). *In Situ* Cell Death Detection Kit was from Boehringer-Mannheim (Indianapolis, IN). ICE-1 inhibitor, zVAD fmk, CPP32 inhibitor, zDEVD fmk, and the nonspecific caspases inhibitor BOCDFK were from Enzyme Systems Products (Dublin, CA). Ferric-NTA complex was prepared as described by Awai *et al.* (1979). Briefly, ferric nitrate was dissolved in 1 N HCl to form a 50 mM solution, and NTA was dissolved in 1 N NaOH to form a 150 mM solution. Equal volumes of the two solutions were mixed just before the experiment, and pH was adjusted to 7.4 with NaHCO₃. The ferric-NTA solution was sterilized by filtration through a 0.45-μm membrane and was used at a ferric/NTA ratio of 1:3. All other chemicals were the highest grade available from commercial supplies. Tissue culture flasks were from Corning Glassworks (Corning, NY).

Culture and treatment of cells. Two human hepatoma HepG2 sublines (Dai *et al.*, 1993) were used in these experiments. HepG2-MV2E1-E9 (E9) cells contain a copy of the human CYP2E1 cDNA and constitutively express CYP2E1. HepG2-MV5 (MV5) cells contain the viral vector lacking the CYP2E1 cDNA. The *p*-nitrophenol oxidation activity of E9 cells was usually at the level of 50–80 pmol/min/mg microsomal protein, and the *p*-nitrophenol oxidase activity of MV5 cells was <2 pmol/min/mg microsomal protein. Cells were cultured at concentrations ranging from 5×10^4 to 1×10^7 cells/ml in MEM containing 5% FBS and 0.1 mg/ml G418 supplemented with 100 units/ml penicillin and 100 μg/ml streptomycin in an incubator in an atmosphere of 5% CO₂/95% air at 37°. Cells were subcultured at a 1:4 ratio once a week. Individual cultures were not maintained for >4–6 weeks. Cell damage was induced by treatment with the Fe-NTA complex at various times and concentrations as indicated in the figure legends.

Cytotoxicity measurement. Cell proliferation and cytotoxicity were determined using an MTT assay (Mosmann, 1983). E9 and MV5 cells were seeded onto 24-well plates at a concentration of 5×10^4 cells/well in 1 ml of MEM plus 5% FBS. After an overnight (12–15 hr) preincubation with or without 0.1 mM BSO, cells were incubated with Fe-NTA for a designated time, most routinely for 12 hr. The medium was removed, and 575 μl of MEM containing 2% FBS and 15% dye solution specific for the MTT assay (Promega MTT Kit) were added for a 1-hr incubation at 37°. Solubilization/stop solution (500 μl/well) was added to each well for an additional 4-hr incubation. The absorbance at 570 nm (formation of formazan) and 630 nm (reference) was recorded with a spectrophotometer (UV 160U; Shimadzu, Kyoto, Japan). The percentage viability was calculated as follows: Viability (%) = $(A_{570} - A_{630})_{\text{SAMPLE}}$ divided by $(A_{570} - A_{630})_{\text{CONTROL}}$ $\times$ 100. Results for individual samples were expressed as a percent of the mean control value in the experiment. LDH activity in cell extracts and released into the medium was assayed spectrophotometrically using the Sigma LDH-20 Diagnostic kit. Cell number was determined directly by counting with the use of a hemocytometer.

Assay of lipid peroxidation. Aldehydes such as MDA and HNE are formed during lipid peroxidation. The concentration of MDA plus HNE was measured by using a lipid peroxide assay kit (Calbiochem-Novabiochem, San Diego, CA). Briefly, 2×10^6 E9 or MV5 cells/ml were cultured in a total volume of 10 ml. The reaction conditions are described in the legends to the figures and tables. After the medium was collected, the cells were removed by scraping in 10 mM Tris·HCl buffer, pH 7.4, containing 0.125 M KCl, followed by low-speed centrifugation. The cell pellets were resuspended in 0.5 ml of Tris·HCl, pH 7.4, and lysed using a sonicator (W-220; Ultrasonic, Farmingdale, NY) under the conditions of duty cycle 25% and output control 40% for 5 sec on ice. The protein concentration of the cell suspension was determined using a protein assay kit (BioRad, Hercules, CA). A 200-μl aliquot of the culture medium or 2 mg of cell lysate protein was assayed for MDA and HNE according to the lipid peroxide assay kit protocol. The absorbance of the sample was monitored at 586 nm, and the concentration of MDA plus HNE or MDA alone was determined from a standard curve.

Assessment of DNA fragmentation. A TUNEL assay was used to detect DNA fragmentation. Briefly, 5×10^6 cells/ml were seeded onto 100-mm petri dishes in a total volume of 6 ml. After incubation, cells were washed twice with PBS (100 mM potassium phosphate, 0.9% NaCl, pH 7.4) containing 1% BSA at 4°, harvested by trypsinization, adjusted to 0.2×10^7 cells/0.2 ml of PBS, and fixed in 4% formaldehyde for 30 min at room temperature. The cells were washed twice with PBS containing 1% BSA and permeabilized with a lysis solution consisting of 0.1% sodium citrate and 0.1% Triton X-100 for 2 min on ice. After washing twice in cold PBS containing 1% BSA, the cells were mixed with fluorescein isothiocyanate-conjugated dUTP in the presence of terminal deoxynucleotidyl transferase enzyme solution or label solution (without terminal transferase) as

negative control and incubated for 1 hr at 37°. After incubation, cells were washed twice in PBS containing 1% BSA and analyzed by flow cytometry, using an EPICS Profile II Analyzer flow cytometer (Coulter, Hialeah, FL).

The DNA fragmentation pattern (DNA laddering) was also assessed by agarose gel electrophoresis. Cells (1×10^6) were scraped and centrifuged at 1200 rpm for 10 min. The cell pellets were resuspended in 1 ml of lysis buffer consisting of 10 mM Tris·HCl, pH 7.4, 10 mM NaCl, 10 mM EDTA, 100 μg/ml proteinase K, and 0.5% SDS and incubated for 1 hr at 50°. DNA was first extracted with 2 ml phenol [balanced with TE buffer (50 mM Tris, 1 mM EDTA, pH 7.5)], followed by extraction with 1 ml of chloroform/isoamylalcohol (24:1). The aqueous phase was precipitated with 2.5 volumes of ice-cold ethanol and 10% volume of 3 M sodium acetate, pH 5.2, at −20° overnight. The precipitates were collected by centrifugation at $13,000 \times g$ for 10 min. The pellets were air-dried and resuspended with 50 μl TE buffer supplemented with 0.1 μg/ml RNase A. DNA was loaded onto a 1.5% agarose gel, electrophoresed in TE buffer containing 2 μg/ml ethidium bromide for 90 min at 90 V, and photographed under UV illumination.

ATP assay. The ATP content of E9 and MV5 cells was determined by the luciferin-firefly luciferase method (Farber, 1982). Briefly, 5×10^4 to 10^6 cells/ml of E9 and MV5 cells were preincubated overnight with 0.1 mM BSO and then incubated with various additions as indicated. The preparation of cell samples was the same as described for the lipid peroxidation assay. Then, 50 μl of cell suspension was assayed for ATP using the Sigma Chemical Luciferase ATP Assay Kit. The contents of ATP were determined from an internal standard curve prepared with ATP.

Oxygen consumption. The respiratory rate of permeabilized cells was measured polarographically with a Clark oxygen electrode (Yellow Springs Instrument, Yellow Springs, OH) in a 3-ml thermo-jacketed chamber with magnetic stirring at 37°C. The cells were first incubated with 0.1 mM BSO overnight. After incubation with buffer or with Fe-NTA for 12 hr, E9 and MV5 cells were harvested by trypsinization, collected by centrifugation at 1200 rpm for 10 min at room temperature, and resuspended at 5×10^6 cells/ml in a total volume of 3 ml of air-saturated buffer consisting of 0.25 M sucrose, 0.1% bovine serum albumin, 10 mM MgCl$_2$, 10 mM K$^+$ HEPES, 1 mM ADP, and 10 mM KH$_2$PO$_4$, pH 7.2. After equilibration for 3–4 min in
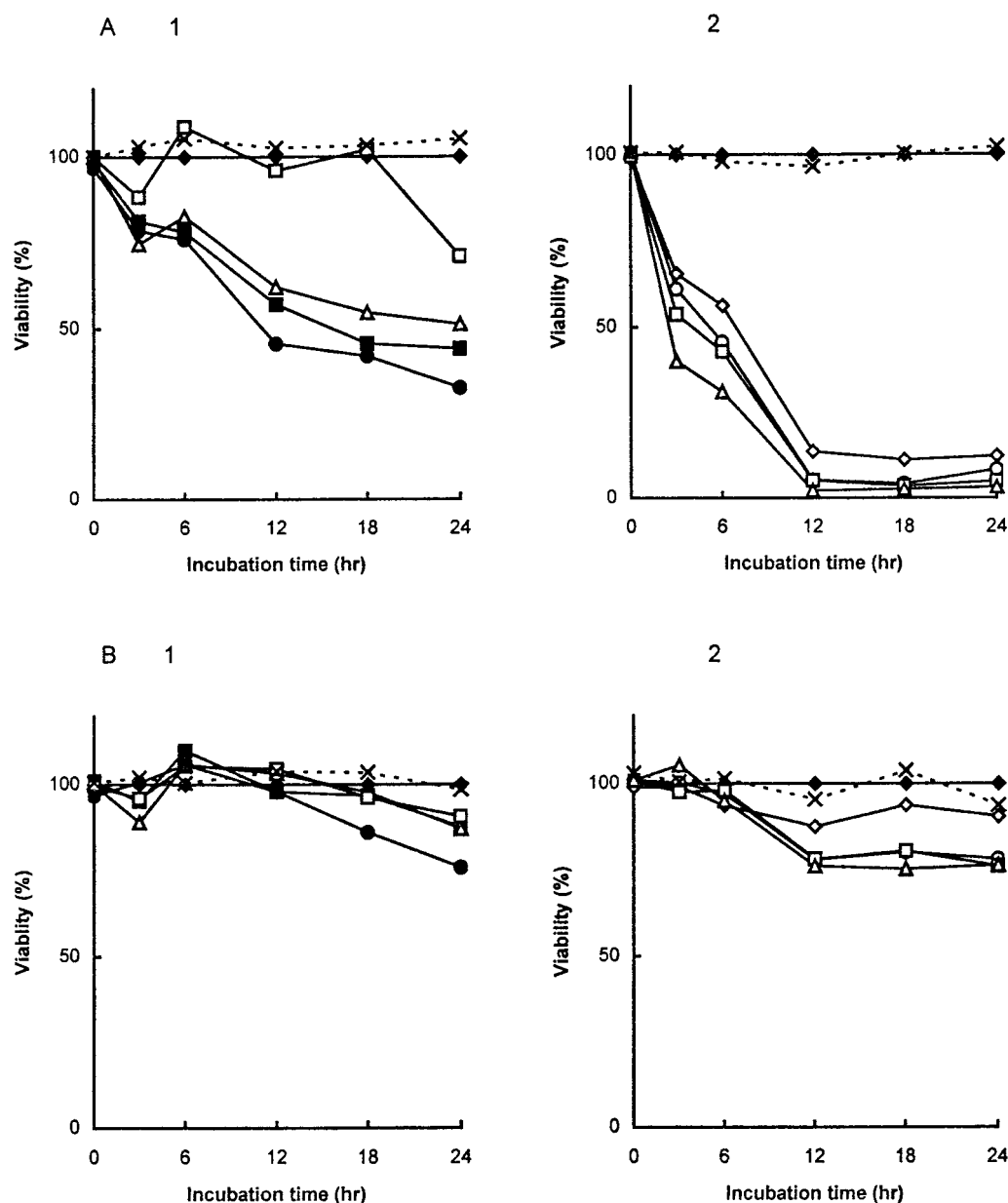
Fig. 1. Dose-response and time course of viability of E9 and MV5 cells treated with Fe-NTA. E9 (A1, A2) and MV5 (B1, B2) cells were preincubated without (A1, B1) or with (A2, B2) 0.1 mM BSO overnight at 37°. After the addition of varying concentrations of Fe-NTA to the culture medium, the cells were incubated for the indicated times, and the viability of the cells was determined by the MTT assay as described in Materials and Methods. *Points*, mean of duplicate samples; a representative experiment is shown. Iron concentrations: ◆, no addition (control); ◇, 15 μM; ○, 30 μM; □, 50 μM; △, 100 μM; ■, 300 μM; and ●, 500 μM. The NTA (×) concentration was either 900 μM for the no BSO treatment experiments or 300 μM for the BSO treatment experiments.

the chamber, the cells were mixed with digitonin (final concentration 0.005%) to permit free entry of mitochondrial substrates and inhibitors. Rates of oxygen uptake were recorded in the presence of substrates and inhibitors as described by Krippner *et al.* (1996). Oxygen concentration was calculated with air-saturated buffer, assuming 217 μM O_2 at 37°.

**Effect of bcl-2 on Fe-NTA toxicity.** Stable HepG2 sublines that were established to overexpress human bcl-2 (Chen and Cederbaum, 1998) were used for these experiments. Transfection of HepG2 cells was carried out using the LipofectAMINE reagent (Life Technologies) as described by Hawley-Nelson *et al.* (1993). The HepG2 cells previously transfected with pCI-Neo, pCI-bcl-2, or pCI-as-bcl-2 were seeded (1.5×10^6) into a 100-mm culture dish and grown until 50–70% confluence. Cells were rinsed with serum-free MEM and pCI-2E1 plasmid DNA, 15 μg, and 100 μl of LipofectAMINE reagent were used to transfect each culture dish of cells. Eighteen hours after transfection, fresh MEM containing 0.8 mg of G418/ml was added and the cells were incubated for an additional 2 days. The cells were harvested by trypsinization for G418 selection and Western blot analysis to detect the presence of CYP2E1 and then exposed to Fe-NTA to assess viability and DNA fragmentation.

Results

Cytotoxic action of Fe-NTA on E9 and MV5 cells. Fig. 1 shows the effect of Fe-NTA on the viability of E9 and MV5 cells. In the absence of BSO, addition of Fe-NTA at concentrations of >0.1 mM to the E9 cell culture medium resulted in a time-dependent inhibition of MTT reduction; the viability of E9 cells was 53 ± 4% after 24-hr exposure to 0.1 mM Fe-NTA. The toxicity of Fe-NTA was much more pronounced in the presence of BSO (e.g., there was 90% inhibition of MTT reduction in E9 cells produced by the addition of 30 μM Fe-NTA after 12 hr) (Fig. 1, A2), indicating that a deficiency in GSH increases the sensitivity of the E9 cells toward the cytotoxic action of Fe-NTA. The decrease in MTT reduction in MV5 cells was not as marked with various incubation times and Fe-NTA concentrations, in the presence or absence of BSO (Fig. 1, B1 and B2) compared with the E9 cells. No

decrease in viability of E9 and MV5 cells was observed when up to 3 mM of NTA alone was added to the culture medium in the presence or absence of BSO, respectively, indicating that it was the iron component of Fe-NTA that induced the cytotoxicity. Similar results showing enhanced cytotoxicity of Fe-NTA to E9 cells compared with MV5 cells were obtained using a LDH leakage assay to assess viability (data not shown). Changes in cell number after incubation with or without Fe-NTA were determined. After incubation with 30 μM Fe-NTA, the number of E9 cells was markedly decreased in a time-dependent manner in the presence of BSO (Fig. 2A). A much smaller decrease was observed in cell number when MV5 cells were treated with Fe-NTA plus BSO (Fig. 2B). After initial plating of 5×10^4 E9 or MV5 cells, followed by a 24-hr incubation with 30 μM Fe-NTA, the number of E9 cells was 3.5×10^3 ($\pm 0.2 \times 10^3$) compared with 3.8×10^4 ($\pm 0.1 \times 10^4$) of MV5 cells. There was no decrease in cell number caused by treatment with NTA only (Fig. 2). These experiments establish that the E9 cells that express CYP2E1 show a much higher sensitivity to Fe-NTA than the MV5 cells that do not express CYP2E1. Because GSH depletion potentiates the Fe-NTA toxicity, subsequent experiments were carried out by first exposing the cells to an overnight (12–15-hr) exposure to 0.1 mM BSO [which lowers GSH levels by 70–90% (Chen *et al.*, 1997)] before the addition of Fe-NTA.

Lipid peroxidation produced by Fe-NTA. Because transition metals such as iron are powerful catalysts of lipid peroxidation processes (Halliwell and Gutteridge, 1984), the production of MDA and HNE on addition of Fe-NTA to E9 or MV5 cells was determined. There was no detectable MDA or HNE in E9 or MV5 cells before the addition of Fe-NTA (Fig. 3). The addition of Fe-NTA resulted in an increase in production of MDA and HNE in extracts of both cell lines (Fig. 3A); however, the increase in these aldehydes was more pronounced with the E9 cells (e.g., at 12 hr), the levels of MDA plus HNE were 5.8 ± 0.2 nmol/mg cell protein for E9 cells compared with values of 1.9 ± 0.1 nmol/mg cell protein for

A

B
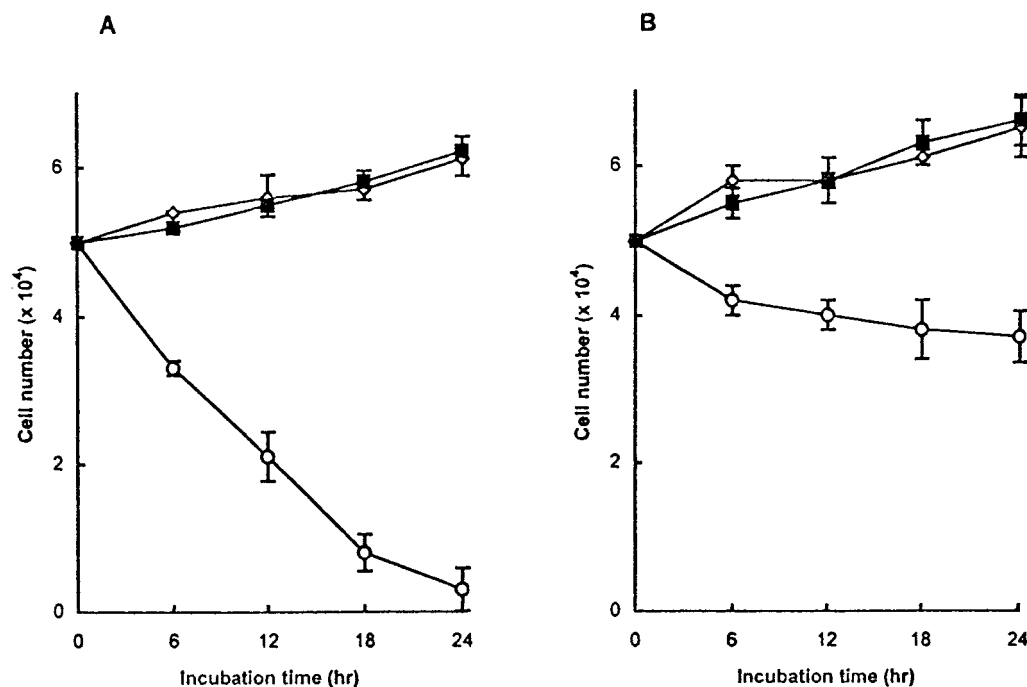
Fig. 2. Cytotoxicity of Fe-NTA to E9 and MV5 cells. E9 (A) and MV5 (B) cells were preincubated overnight with 0.1 mM BSO. After the addition of 90 μM NTA or 30 μM Fe-NTA to the culture medium, the cells were incubated for the indicated times, and cell number was counted as described in Materials and Methods. *Points*, mean ± standard error of triplicate experiments. ■, No addition (control); ○, 30 μM Fe-NTA; ◇, 90 μM NTA.

MV5 cells ($p < 0.05$). MDA could be detected in the culture medium of the cells after treatment with Fe-NTA, and more MDA was present in the medium from E9 cells than the MV5 cells although these differences (50%) were not as pronounced as the 3-fold differences found intracellularly (Fig. 3B).

Vitamin E and vitamin E analogues such as Trolox are powerful inhibitors of lipid peroxidation. When these agents were added to the E9 cell tissue culture medium, the Fe-NTA-induced increase in MDA and HNE levels, in cell extracts as well as released to the medium, was strongly inhibited (Fig. 4).

Effect of antioxidants on Fe-NTA toxicity to E9 cells. Because Fe-NTA promoted a large increase in lipid peroxidation of E9 cells, the effect of a variety of antioxidants on the Fe-NTA-induced loss of cell viability was determined. Vitamin E and Trolox completely prevented the Fe-NTA cytotoxicity (Table 1). Ascorbate was partially protective at a 0.2 mM concentration but became less effective at a higher concentration; this may reflect the antioxidant versus prooxidant

action of ascorbate in biological systems, especially in the presence of transition metals. A small protective effect was observed in the presence of catalase but not SOD (Table 1). DMSO and 4-methylpyrazole, which are ligands for CYP2E1 and inhibit CYP2E1 catalytic function (Eliasson *et al.*, 1988), also afforded a small protective effect; these compounds also are powerful hydroxyl radical scavenging agents, which may contribute to their protective effect. The effect of ethanol, also a hydroxyl radical scavenger, will be the subject of future studies; ethanol may be protective or may promote toxicity by increasing the CYP2E1 content. Thiourea or *N*-acetylcysteine, nonspecific radical scavengers, however, had no protective effect at the levels used (Table 1). The most effective antioxidants to provide protection against the Fe-NTA-induced cytotoxicity to E9 cells were vitamin E and Trolox, which also were strongly protective against the Fe-NTA-induced lipid peroxidation.

Effect of Fe-NTA on mitochondrial oxygen consumption. Experiments were carried out to evaluate whether one potential consequence of the Fe-NTA catalyzed lipid peroxi-
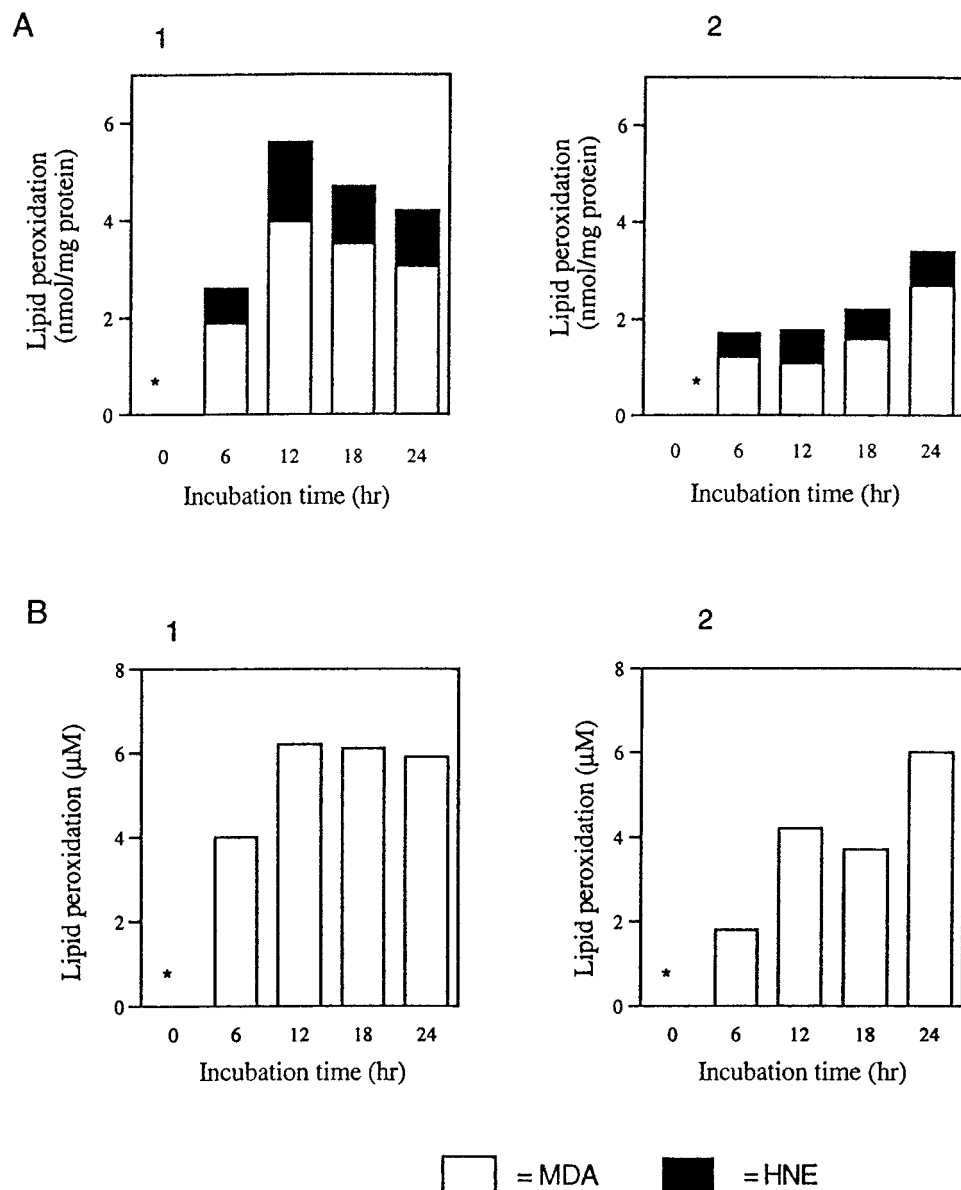
Fig. 3. Time course of lipid peroxidation in Fe-NTA-treated E9 and MV5 cells. After an overnight incubation with 0.1 mM BSO, E9 (A1, B1) and MV5 (A2, B2) cells were incubated with 30 μM Fe-NTA for the indicated times. MDA ($\square$) and HNE ($\blacksquare$) were measured in cell extracts (A1, A2) and culture medium (B1, B2) as described in Materials and Methods. Results are from three experiments. *, Not detectable.

dation in E9 cells was an effect on mitochondrial function, with a subsequent loss of ATP production. Oxygen uptake by digitonin-permeabilized E9 and MV5 cells that had previously been incubated with 30 μM Fe-NTA for 12 hr was studied using substrates that donate electrons to complex I (pyruvate/malate), complex II (succinate), and complex IV (ascorbate/tetramethyl-p-phenylenediamine) of the respiratory chain (Krippner *et al.*, 1996). Oxygen uptake through the
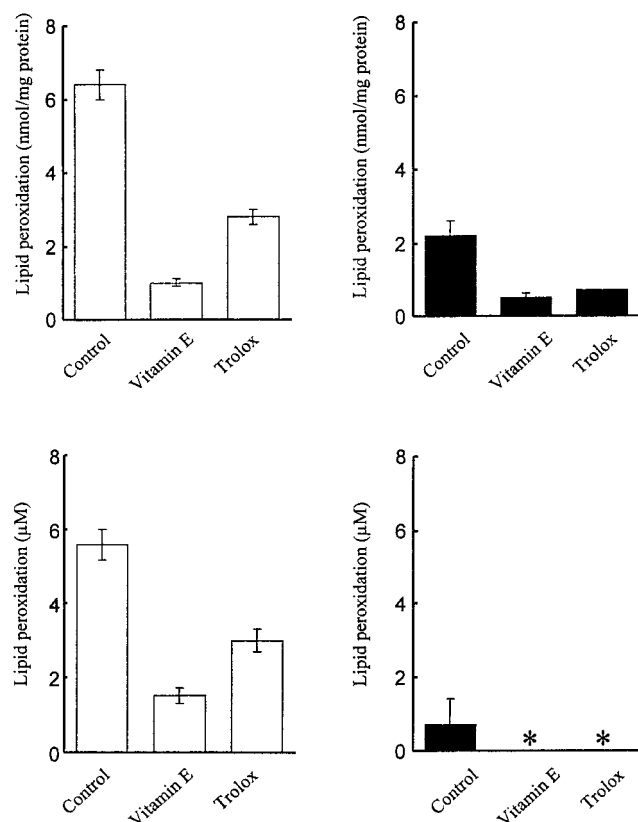
Fig. 4. Protective effect of vitamin E and Trolox against lipid peroxidation in E9 cells treated with Fe-NTA. E9 cells were incubated with 30 μM Fe-NTA for 12 hr in the presence or absence of 25 μM of vitamin E or 50 μM of Trolox. MDA (□) and HNE (■) were measured in cell extracts (*top*) and culture medium (*bottom*) as described in Materials and Methods. Data represent the mean ± standard error of triplicate experiments. ∗, Not detectable.

Fig. 5. Effect of Fe-NTA on mitochondrial electron transfer in E9 and MV5 cells. E9 (*traces 1* and *2*) and MV5 (*traces 3* and *4*) cells were treated with 0.1 mM BSO overnight and then incubated with (*traces 1* and *3*) or without (*traces 2* and *4*) 30 μM Fe-NTA for 12 hr. The cells were harvested, and measurements of oxygen consumption were performed in a respiration buffer, pH 7.2, containing 1 mM ADP as described in Materials and Methods. Additions (*arrows*) included digitonin (0.005%), malate (5 mM)/pyruvate (5 mM), rotenone (0.1 μM), succinate (5 mM), antimycin A (0.05 μM), ascorbate (1 mM)/tetramethyl-p-phenylenediamine (0.4 mM), and azide (5 mM). The concentration in parentheses is the final concentration of the addition. *Traces* from a typical experiment are shown; similar results were obtained in three other experiments and are summarized in Table 2.
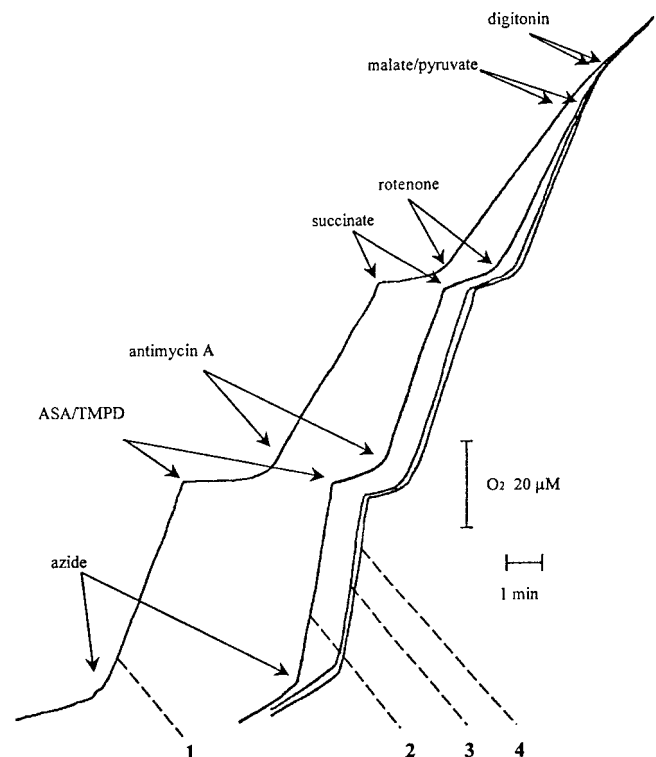
TABLE 1

Effect of various compounds on the cytotoxicity produced by Fe-NTA to E9 cells

After an overnight incubation with 0.1 mM BSO, E9 cells (5×10^4 cells/ml) were incubated with or without 30 μM Fe-NTA in the presence or absence of the indicated additions. The viability of the cells was determined by the MTT assay. Each value represents the mean ± standard error of three experiments.
The control change in absorbance ($A_{570} - A_{630}$) was 0.590 ± 0.008, which is taken as 100% viability.

Addition	Viability	
	−Fe-NTA	+Fe-NTA
	%	
None (control)	100 ± 1.1	10.4 ± 1.1
0.01 mM Vitamin E	104.1 ± 2.3	84.1 ± 2.6[a]
0.025 mM Vitamin E	99.4 ± 1.9	103.2 ± 4.5[a]
0.025 mM Trolox	91.9 ± 1.7	94.2 ± 3.4[a]
0.05 mM Trolox	91.2 ± 2.3	102.1 ± 0.6[a]
0.2 mM Ascorbate	96.2 ± 2.1	43.2 ± 3.0[a]
1.0 mM Ascorbate	104.3 ± 5.6	26.0 ± 3.2[a]
1000 units/ml SOD	83.6 ± 2.8	9.6 ± 1.7
2000 units/ml Catalase	83.7 ± 1.9	44.9 ± 1.9[a]
5 mM Thiourea	85.3 ± 0.9	5.8 ± 0.6
4 mM *N*-acetylcysteine	84.8 ± 0.4	7.8 ± 1.2
4 mM 4-Methylpyrazole	100.4 ± 0.4	41.0 ± 1.7[a]
25 mM DMSO	107.1 ± 3.6	38.0 ± 3.4[a]

[a] $p < 0.05$ compared with Fe-NTA-treated E9 cells in the absence of any addition.

TABLE 2

Effect of Fe-NTA on oxygen consumption in E9 and MV5 cells

After an overnight incubation with 0.1 mM BSO, E9 or MV5 cells (5×10^6 cells/ml) were incubated with or without 30 μM Fe-NTA and with or without 0.025 mM vitamin E for 12 hr. The cells were harvested and oxygen consumption was assayed as described in Materials and Methods and the legend to Fig. 5. Values represent the mean ± standard error of three experiments.

Cells Addition	Oxygen uptake		
	Pyr/Mal	Succinate	Asc-TMPD
	nmol/min/5×10^6 cells		
E9			
None	18.9 ± 2.2	21.8 ± 1.6	41.0 ± 1.9
Fe-NTA	11.7 ± 2.2[a]	11.9 ± 2.3[a]	19.9 ± 2.5[a]
Vitamin E	19.2 ± 0.5	20.2 ± 0.8	40.7 ± 0.8
Vitamin E and Fe-NTA	18.9 ± 1.7	18.8 ± 2.7	36.6 ± 1.9
MV5			
None	21.0 ± 0.8	24.2 ± 0.8	47.9 ± 1.1
Fe-NTA	20.2 ± 0.8	24.8 ± 0.9	46.8 ± 1.0
Vitamin E	21.4 ± 2.5	23.9 ± 0.8	48.0 ± 0.5
Vitamin E and Fe-NTA	21.1 ± 0.2	22.1 ± 1.0	44.0 ± 0.6

[a] $p < 0.05$ compared with the control E9 cells.

various complexes was segregated by the use of inhibitors such as rotenone (complex I), antimycin A (complex III), and azide (complex IV). The rate of oxygen uptake by E9 cells was similar to that of the MV5 cells with all three substrates (Fig. 5, *traces 2* and *4*; Table 2) in the absence of the Fe-NTA treatment. Treatment with Fe-NTA resulted in a decreased rate of oxygen consumption by the E9 cells with all three substrates (Fig. 5, *trace 1*; Table 2). However, the Fe-NTA

TABLE 3
Effect of Fe-NTA on ATP levels in E9 and MV5 cells
E9 or MV5 cells (0.5×10^6 cells/ml) were treated with 0.1 mM BSO for 15 hr and then were incubated with or without 30 μM Fe-NTA and the indicated additions for 12 hr. Levels of ATP were determined as described in Materials and Methods. Results represent the mean ± standard error of 4–12 experiments.

| Cells Addition	ATP content		Effect of Fe-NTA
	−Fe-NTA	+Fe-NTA	
	pmol / mg protein		*(%)*
E9			
None	9.4 ± 1.0	5.9 ± 0.8	−37[a]
0.025 mM Vitamin E	10.5 ± 0.6	9.0 ± 1.3	−14
0.05 mM Trolox	9.8 ± 1.3	10.2 ± 1.3	+4
MV5			
None	13.6 ± 0.7	11.0 ± 1.1	−19
0.025 mM Vitamin E	12.4 ± 0.2	12.0 ± 0.9	−3
0.05 mM Trolox	12.9 ± 0.6	11.5 ± 0.2	−11

[a] $p < 0.05$.

treatment did not affect the rate of oxygen uptake by the MV5 cells (Fig. 5, *trace 3*). The presence of 0.025 mM vitamin E during the 12-hr treatment period before measuring oxygen consumption had no effect on rates of oxygen uptake in the absence of Fe-NTA but completely prevented the inhibition produced by Fe-NTA in the E9 cells (Table 2).

Because inhibition of oxygen consumption should affect rates of ATP production, the levels of ATP in E9 and MV5 cells were determined. The ATP levels in E9 cells, in the absence of Fe-NTA treatment, were ~25% lower than the levels in the MV5 cells (Table 3). Treatment with 30 μM Fe-NTA for 12 hr resulted in a 37% decline in the ATP levels of the E9 cells, similar to the 40–50% decrease in rates of oxygen consumption produced by Fe-NTA (Tables 2 and 3). A smaller, nonstatistically significant decrease in ATP levels was produced by Fe-NTA with the MV5 cells. After treatment with Fe-NTA, ATP levels in the E9 cells were only half those of the MV5 cells (Table 3). The decrease in ATP levels produced by Fe-NTA was prevented by vitamin E and by Trolox (Table 3).

Fe-NTA-induced DNA fragmentation. Intracellular reactive oxygen species and elevated levels of lipid peroxidation have been implicated as being associated with DNA fragmentation and apoptosis (Hockenberry *et al.*, 1993; Reed, 1994). To determine whether Fe-NTA produced DNA fragmenta-
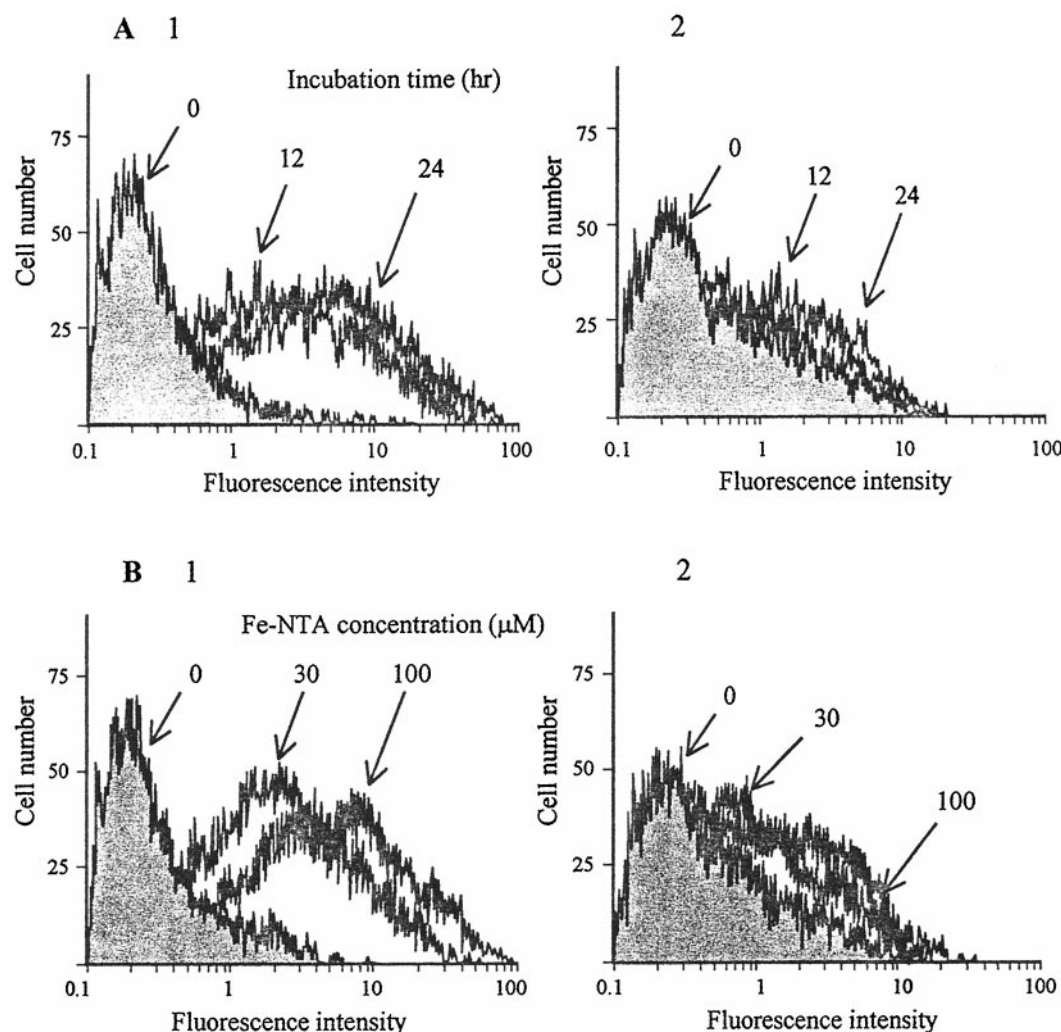
Fig. 6. DNA fragmentation in E9 and MV5 cells after treatment with Fe-NTA. After an overnight incubation with 0.1 mM BSO, E9 (A, 1, B, 1) and MV5 (A, 2, B, 2) cells were incubated with 30 μM Fe-NTA for either 12 or 24 hr (*arrows*, A1 and A2) or with either 30 or 100 μM of Fe-NTA for 12 hr (*arrows*, B1 and B2). The DNA fragmentation was measured by the TUNEL method as described in Materials and Methods. Similar results were observed in two other independent experiments using two different preparations of cells.

tion, the TUNEL assay and DNA ladder formation were used as indices of DNA fragmentation. Treatment of E9 cells with 30 μM Fe-NTA for 12 or 24 hr resulted in enhanced fluorescence (Fig. 6, A1), whereas little effect was observed with the MV5 cells (Fig. 6, A2). Treatment of the MV5 cells for 12 hr with concentrations of Fe-NTA as high as 100 μM resulted in only a modest increment in DNA fragmentation (Fig. 6B, *2*), whereas the fluorescence intensity was markedly increased with the E9 cells (Fig. 6, B1). Essentially, similar results were observed with respect to DNA ladder formation. Treatment of the E9 cells with 30 μM Fe-NTA resulted in a time-dependent DNA ladder formation (Fig. 7A, *lanes 1–4*), whereas no DNA ladder could be observed in MV5 cells even after 24-hr treatment with 30 μM Fe-NTA (Fig. 7A, *lanes 5–8*) or after 12-hr treatment with Fe-NTA concentrations of 30, 50, or 100 μM (Fig. 7B, *lanes 6–8*).

The effect of a variety of antioxidative agents on the Fe-NTA-induced DNA ladder formation in the E9 cells is shown in Fig. 8. The following agents provided strong protection against DNA ladder formation: vitamin E, Trolox, ascorbate, catalase, the spin-trapping agent N-t-butyl-α-phenylnitrone, 4-methylpyrazole, and DMSO. No protection against DNA ladder formation was afforded by SOD, thiourea, or N-acetylcysteine (Fig. 8).

It is of interest that some of the reagents that strongly protect against DNA fragmentation (ascorbate, catalase, DMSO) or bcl-2 (see below) only partially protected against loss of cell viability (Table 1). Whether this reflects induction by Fe-NTA of both necrotic and apoptotic modes of cell death or toxicity due to several mechanisms (DNA fragmentation, mitochondrial damage, decreased ATP) is not known.

Effect of bcl-2 on Fe-NTA-induced cytotoxicity in E9 cells. The proto-oncogene bcl-2 has been shown to prevent DNA fragmentation under a variety of conditions (Hockenberry *et al*., 1993; Merino *et al*., 1994; Reed, 1994). To assess the effect of bcl-2 on the Fe-NTA-induced loss of viability in CYP2E1-expressing cells, stable HepG2 cell lines that express or do not express bcl-2 were established by transfection with pCI-Neo plasmid or pCI-Neo containing human bcl-2 in the sense or the antisense orientation, followed by G418 selection and limited dilution to yield monoclones (Chen and Cederbaum, 1998). These cells were transfected with pCI-2E1 plasmid and, 2 days after transfection, incubated with

Fe-NTA and analyzed for viability and DNA ladder formation. Immunoblots indicated a low level of bcl-2 in the pCI-Neotransfected cells, a nondetectable level of bcl-2 in the pCI-as-bcl-2-transfected cells, and a ~10-fold enrichment of bcl-2 in the pCI-sense-bcl-2-transfected cells (data not shown but similar to that reported in Fig. 9 of Chen and Cederbaum, 1998). Immunoblots indicated the levels of CYP2E1 were similar in the three cell lines 2 days after transfection with the pCI-2E1 plasmid (data not shown but similar to that reported in Fig. 9 of Chen and Cederbaum, 1998). As shown in Fig. 9, the toxicity of 30 μM Fe-NTA was less pronounced over a 24-hr time course to the bcl-2 overexpressing HepG2 cells compared with the control cells or the cells that do not express bcl-2. Interestingly, although strong differences in susceptibility to Fe-NTA between the bcl-2 overexpressing cells and the other two cell lines were observed at 30 μM Fe-NTA, these differences became less pronounced as the concentration of Fe-NTA was elevated (i.e., bcl-2 was less protective against toxicity produced by high concentrations of Fe-NTA) (Fig. 9).

After transfection with pCI-CYP2E1 plasmid and after incubation with 30 μM Fe-NTA for 12 hr, DNA ladder formation was observed in the pCI-control HepG2 cells and the cells that do not express bcl-2 (Fig. 10, *lanes 1* and *3*, respectively). However, DNA ladder formation was much less pronounced in the cells that overexpress bcl-2 (Fig. 10, *lane 2*).

Effect of an inhibitor of caspase 3 on Fe-NTA toxicity in E9 cells. DNA fragmentation often is associated with the activation of a family of cysteine proteases, the caspases, and caspase 3, CPP32, seems to play an important role in several models of apoptosis (Martin and Green, 1995; Thompson, 1995). The effect of zDEVD fmk, an inhibitor of caspase 3, on the Fe-NTA-induced toxicity and DNA fragmentation was evaluated. LDH release by E9 cells over a 24-hr incubation was increased by Fe-NTA (Fig. 11). This increase was completely blocked by zDEVD fmk (Fig. 11). In a similar manner, DNA ladder formation produced by treatment of E9 cells with 30 μM Fe-NTA (Fig. 12, *lane 2*) was decreased by 50 μM (but not 5 μM) zDEVD fmk (Fig. 12, *lanes 6* and *7*). However, inhibitors of caspase 1 such as zVAD fmk or BOCDFK did not prevent the Fe-NTA-induced DNA ladder formation (Fig. 12,
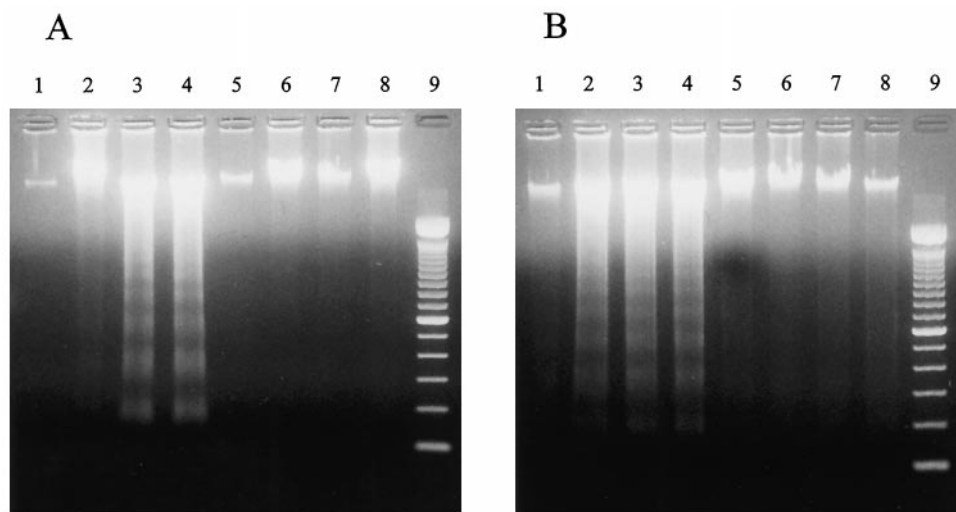
Fig. 7. Dose-response and time course of DNA ladder formation in E9 and MV5 cells treated with Fe-NTA. E9 and MV5 cells were first treated with 0.1 mM BSO for 15 hr. A, E9 (*lanes 1–4*) and MV5 (*lanes 5–8*) cells were incubated with 30 μM Fe-NTA for 0, 6, 12, and 24 hr (*lanes 1* and *5*, *2* and *6*, *3* and *7*, *4* and *8*, respectively). *Lane 9*, 200-bp DNA marker. B, E9 (*lanes 1–4*) and MV5 (*lanes 5–8*) cells were incubated for 12 hr with 0, 30, 50, and 100 μM Fe-NTA (*lanes 1* and *5*, *2* and *6*, *3* and *7*, *4* and *8*, respectively). *Lane 9*, 200-bp DNA marker. DNA was isolated and electrophoresed as described in Materials and Methods. Similar results were observed in two other independent experiments using different preparations of cells.
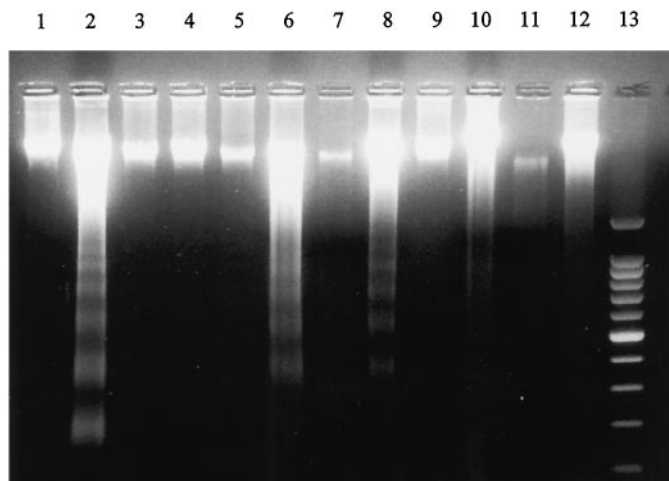
lanes 3, 4, 9, and *10*). No DNA ladder formation was observed in the absence of Fe-NTA (Fig. 12, *lanes 1, 5, 8,* and *11*).
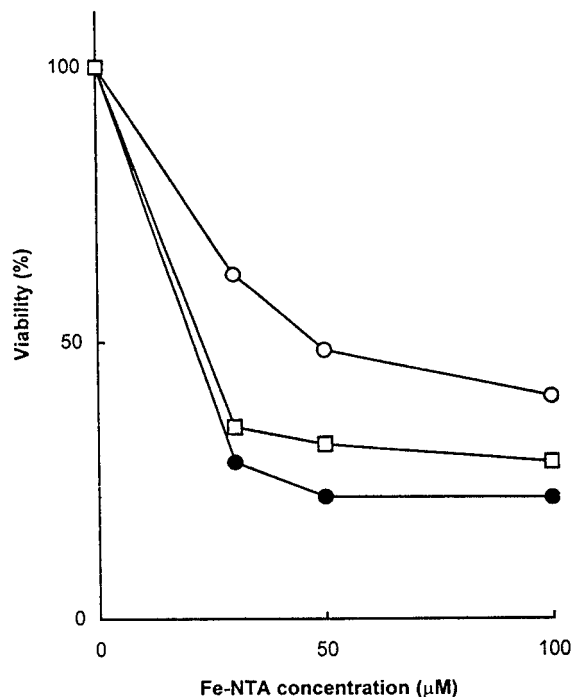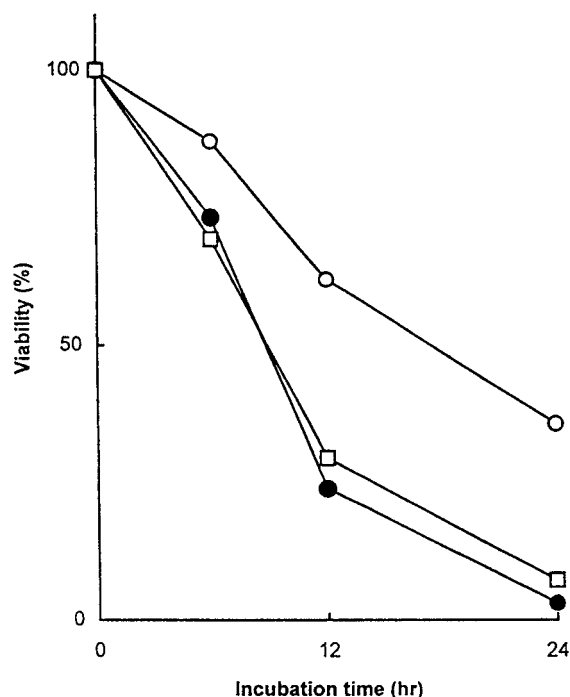
Discussion

Iron has been shown to potentiate the toxicity produced by acute or chronic administration of ethanol. Experiments were carried out in HepG2 cells that express CYP2E1 to

Fig. 8. Effect of various compounds on DNA ladder formation in E9 cells treated with Fe-NTA. E9 cells were incubated for 12 hr with the following additions. *Lane 1,* buffer control. *Lanes 2–12,* from samples that were incubated with 30 μM Fe-NTA plus the following: *lane 2,* no further addition; *lane 3,* 25 μM vitamin E; *lane 4,* 50 μM Trolox; *lane 5,* 0.2 mM ascorbate; *6,* 1000 units/ml SOD; *lane 7,* 2000 units/ml catalase; *lane 8,* 5 mM thiourea; *lane 9,* 1 mM *N-t*-butyl-α-phenylnitrone; *lane 10,* 4 mM *N*-acetylcysteine; *lane 11,* 4 mM 4-MP; *lane 12,* 25 mM DMSO. *Lane 13,* 200-bp DNA marker.

attempt to link CYP2E1, iron, oxidative stress, and cytotoxicity as a potential mechanism by which iron potentiates ethanol toxicity. The addition of iron as an Fe-NTA complex resulted in cytotoxicity to the HepG2 cells expressing CYP2E1, whereas little toxicity was observed in the HepG2 cells not expressing CYP2E1. Thus, expression of CYP2E1 or the addition of Fe-NTA to cells not expressing CYP2E1 had little effect on cell viability, whereas the combination of CYP2E1 expression plus Fe-NTA resulted in pronounced toxicity. The Fe-NTA toxicity was accompanied by DNA fragmentation as assessed by TUNEL analysis and DNA ladder formation and was reduced by bcl-2 and an inhibitor of caspase 3. Although these observations may be suggestive of apoptosis as one mode of Fe-NTA-induced cell death, more detailed studies, including morphological assessment, will be required to evaluate this.

Lipid peroxidation seems to play a central role in the CYP2E1 plus Fe-NTA-dependent induction of toxicity in that vitamin E and Trolox completely prevented the cytotoxicity, and lipid peroxidation caused by Fe-NTA was more pronounced in the E9 cells compared with the MV5 cells. Catalase, but not SOD, afforded some protection, suggesting an important role for H_2O_2 in the developing lipid peroxidation and toxicity. It is not clear whether the catalase is operative intracellularly or extracellularly; uptake of catalase by hepatocytes by an endocytosis-dependent mechanism has been demonstrated (Kyle *et al.*, 1988). Alternatively, because H_2O_2 is diffusible, extracellular catalase may function as an extracellular sink, helping to remove H_2O_2 that is generated intracellularly. One important role for H_2O_2, especially in the presence of iron, could be the production of hydroxyl radical or ferryl-type oxidants, which are powerful initiators of lipid peroxidation. The partial protection against cytotoxicity by

Fig. 9. Protective effect of bcl-2 against Fe-NTA-induced cytotoxicity. HepG2-Neo ($\square$), HepG2-bcl-2 ($\bigcirc$), and HepG2 antisense bcl-2 ($\bullet$) were transfected with pCI-2E1 plasmid to express CYP2E1 (validated by immunoblots). Two days after the CYP2E1 transfection, the cells were treated with 0.1 mM BSO for 15 hr and then were incubated with 30 μM Fe-NTA for varying times or incubated with various concentrations of Fe-NTA for 12 hr before the MTT assay. *Points,* mean of duplicate experiments. The control change in absorbance for the 12-hr incubation in B ($A_{570} - A_{630}$) was 0.336 and 0.314 with the average (0.325) taken as 100% viability.

DMSO or 4-methylpyrazole may be due in part to the ability of these agents to react with hydroxyl radical-like species. Taken as a whole, these results suggest that elevated generation of reactive oxygen species in HepG2 cells expressing CYP2E1 can lead to enhanced lipid peroxidation in the presence of iron, and the ensuing prooxidative state results in loss of cell viability.

Caspase 3 seems to play an important role in the CYP2E1 plus Fe-NTA-dependent loss of cell viability because a relatively specific peptide inhibitor of caspase 3 prevented the cytotoxicity and the DNA fragmentation. In contrast, two inhibitors of caspase 1 did not block DNA ladder formation. Caspase 3 (CPP32) is expressed as a 32-kDa precursor that is processed by proteolytic cleavage to active 17- and 12-kDa forms (Enari *et al*., 1996). This processing is activated by apoptotic-inducing factors, including cytochrome *c*, which can be released when mitochondria lose their membrane potential (Liu *et al*., 1996; Zamzami *et al*., 1996). Future studies will evaluate whether caspase 3 is activated after treatment of E9 cells with Fe-NTA and attempt to assay for release of cytochrome *c* or other apoptotic inducing factors into the cytosol of these cells.

The proto-oncogene bcl-2 inhibits many types of apoptotic cell death, although the mechanism is not clear (Hockenberry

et al., 1993; Reed, 1994). One function of bcl-2 has been suggested to be that of an antioxidant (Hockenberry *et al*., 1993); bcl-2 is found in the mitochondria, and recent studies have shown that bcl-2 may prevent apoptosis by inhibiting the release of apoptotic-inducing factors, notably cytochrome *c*, from the mitochondria (Liu *et al*., 1996). Fe-NTA was considerably less toxic to the HepG2 cells overexpressing bcl-2 compared with the cell lines treated with plasmid alone or with antisense bcl-2. DNA ladder formation induced by Fe-NTA was not observed in the bcl-2-overexpressing cells. Thus, bcl-2 prevents or decreases the Fe-NTA-induced toxicity.

Chronic ethanol treatment has been shown to cause damage to mitochondrial function (Cederbaum *et al*., 1974; Spach and Cunningham, 1987), and lipid peroxidation of mitochondria occurs after ethanol intake (Kamimura *et al*., 1992; Kukielka *et al*., 1994). The treatment of HepG2 cells that do not express CYP2E1 with 30 μM Fe-NTA for 12 hr had no effect on oxygen uptake by permeabilized cells with substrates donating electrons to complex I, II, or IV of the mitochondrial respiratory chain. However, similar treatment of HepG2 cells that do express CYP2E1 resulted in 40–50% decreases in the rates of oxygen uptake with all substrates that can be prevented by vitamin E. Associated with the decreased rates of oxygen consumption after Fe-NTA treatment was a corresponding decline in cellular ATP levels, which can be prevented by inhibitors of lipid peroxidation. The mitochondrial damage and the cellular toxicity are linked by their dependence on lipid peroxidation-dependent reactions.

Recent studies have implicated mitochondria in apoptosis because loss of membrane potential and mitochondrial permeability transition and swelling seem to occur in the early phase of apoptosis. Such affected mitochondria release factors that seem to activate caspases, including an apoptotic-inducing factor and cytochrome *c* (Liu *et al*., 1996; Zamzami *et al*., 1996). It is interesting to speculate that the impairment of mitochondrial function when Fe-NTA is added to the CYP2E1-expressing cells may result in release of apoptotic
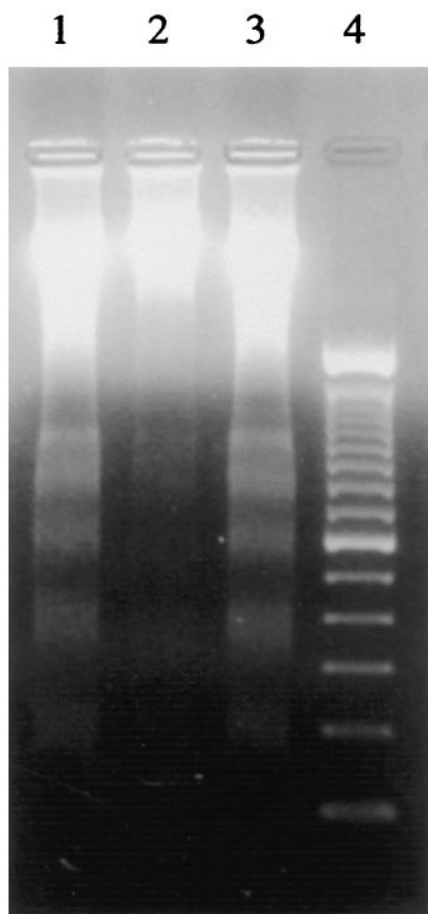

Fig. 10. Protective effects of bcl-2 against Fe-NTA-induced DNA ladder formation. HepG2-Neo (*lane 1*), HepG2-bcl-2 *(lane 2)*, and HepG2 antisense bcl-2 *(lane 3)* cells, which were transfected with pCI-2E1 to express CYP2E1, were incubated with 30 μM Fe-NTA for 12 hr. DNA was isolated and electrophoresed as described in Materials and Methods. *Lane 4*, 200-bp DNA marker
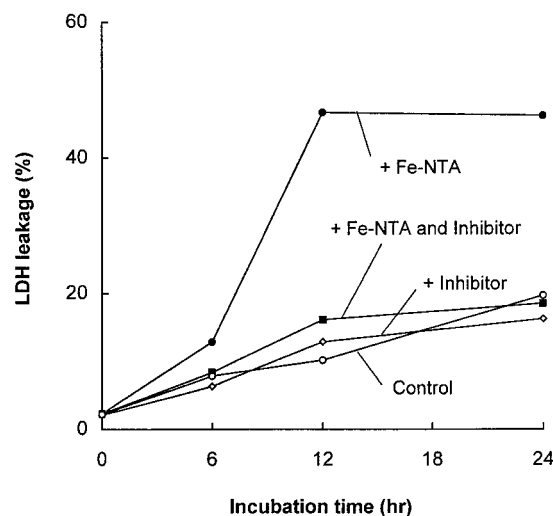

Fig. 11. Effect of the caspase 3 inhibitor, zDEVD fmk, on LDH leakage from E9 cells induced by Fe-NTA. After an overnight incubation with 0.1 mM BSO, E9 cells were incubated with or without 30 μM Fe-NTA for the indicated times, in the absence or presence of 50 μM zDEVD fmk. The inhibitor was added 1 hr before the addition of Fe-NTA.

inducing factors or activators of caspase 3. Studies are planned to evaluate this possibility in the E9 and MV5 cells, as well as in the cell lines that overexpress bcl-2.

Ethanol has been shown to produce liver apoptosis after
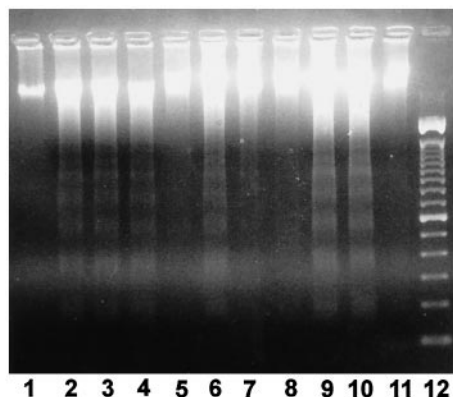
Fig. 12. Effect of inhibitors of caspases 1 and 3 on DNA ladder formation induced by Fe-NTA in E9 cells. E9 cells were incubated for 12 hr with the following: *lane 1*, no additions (control); *lane 2*, 30 μM Fe-NTA; *lane 3*, Fe-NTA plus 5 μM zVAD fmk; *lane 4*, Fe-NTA plus 50 μM zVAD fmk; *lane 5*, 50 μM zVAD fmk; *lane 6*, Fe-NTA plus 5 μM zDEVD fmk; *lane 7*, Fe-NTA plus 50 μM zDEVD fmk; *lane 8*, 50 μM zDEVD fmk; *lane 9*, Fe-NTA plus 5 μM BOCDFK; *lane 10*, Fe-NTA plus 50 μM BOCDFK; *lane 11*, 50 μM BOCDFK; *lane 12*, DNA 200-bp marker. DNA ladder formation was assayed as described in Materials and Methods.
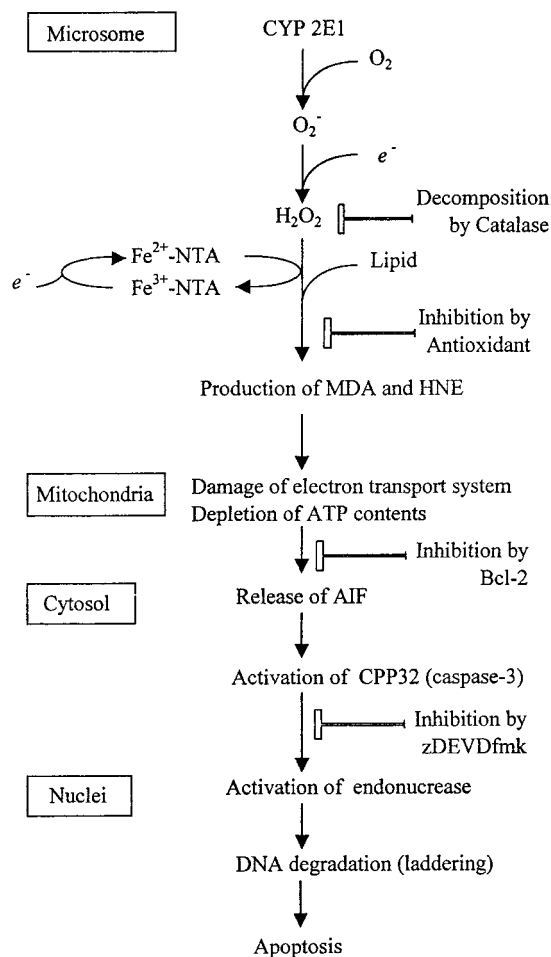
Fig. 13. Hypothetical scheme for cytotoxicity induced by Fe-NTA in E9 cells.

long-term consumption by mice or rats (Benedetti *et al.*, 1988) or when added to isolated rat hepatocytes (Kurose *et al.*, 1997). Apoptotic cells were observed in the livers of rats that exhibited alcohol liver injury (Yacoub *et al.*, 1995). The mechanism by which ethanol causes apoptosis is not clear, although an oxidant-dependent mechanism was suggested in the isolated hepatocyte system (Kurose *et al.*, 1997). Although expression of CYP2E1 alone (at the levels found in E9 cells) or addition of Fe-NTA to cells not expressing CYP2E1 has little effect on cellular viability, the combination of CYP2E1 expression plus Fe-NTA resulted in pronounced toxicity and DNA fragmentation. These results raise the interesting speculation that ethanol-mediated induction of CYP2E1 coupled to an ethanol-induced increase in nonheme iron levels in the liver may be a potential mechanism by which ethanol causes oxidative stress and hepatotoxicity.

A proposed model for the results presented in this work is shown in Fig. 13. CYP2E1 produces reactive oxygen intermediates such as O_2^- and H_2O_2 as a consequence of oxygen activation. In the presence of an iron catalyst, the enhanced generation of reactive oxygen species eventually results in lipid peroxidation as evident by the increased production of MDA and HNE. Lipid hydroperoxides or reactive lipid aldehydes damage the mitochondria, as shown by decreased rates of oxygen consumption and lowered levels of ATP. Apoptotic inducing factors are released from the damaged mitochondria, which activate caspase 3 and results in DNA fragmentation. The general scheme is reasonably consistent with the protection against toxicity that is provided by catalase (removes H_2O_2), by antioxidants (prevent lipid peroxidation), by bcl-2 (prevents lipid peroxidation and prevents release of apoptotic inducing factors), and by zDEVD fmk (inhibits caspase 3). Further studies are required to validate the scheme (e.g., loss of mitochondrial membrane potential, mitochondrial permeability transition, release of apoptotic inducing factors, activation of caspase 3, and potential role of other caspases). These results suggest that one mechanism by which iron may potentiate ethanol hepatotoxicity may be related to the production of a state of oxidative stress and enhanced lipid peroxidation as a consequence of the interaction of iron with CYP2E1-derived reactive oxygen species.

References

Awai M, Narasaki M, Yamanoi Y, and Seno S (1979) Induction of diabetes in animals by parenteral administration of ferric nitrilotriacetate. *Am J Pathol* **95:**663–674.

Benedetti A, Brunelli E, Risicato R, Cillufo T, Jezequel AM, and Orlandi F (1988) Subcellular changes and apoptosis induced by ethanol in rat liver. *J Hepatol* **6:**137–143.

Castillo T, Koop DR, Kamimura S, Triadafilopoulos G, and Tsukamoto H (1992) Role of cytochrome P4502E1 in ethanol-CCl₄ and iron-dependent microsomal lipid peroxidation. *Hepatology* **16:**992–996.

Cederbaum AI (1989) Oxygen radical generation by microsomes: role of iron and implications for alcohol metabolism and toxicity. *Free Radical Biol Med* **7:**559–567.

Cederbaum AI, Lieber CS, and Rubin E (1974) Effects of chronic ethanol treatment on mitochondrial function: damage to complex I. *Arch Biochem Biophys* **165:**560–569.

Chen Q and Cederbaum AI (1998) Cytotoxicity and apoptosis produced by cytochrome P4502E1 in HepG2 cells. *Mol Pharmacol* **53:**638–648.

Chen Q, Galleano M, and Cederbaum AI (1997) Cytotoxicity and apoptosis produced by arachidonic acid in HepG2 cells over-expressing human cytochrome P4502E1 *J Biol Chem* **272:**14532–14541.

Dai Y, Rashba-Step J, and Cederbaum AI (1993) Stable expression of human cytochrome P4502E1 in HepG2 cells: characterization of catalytic activities and production of reactive oxygen intermediates. *Biochemistry* **32:**6928–6937.

Ekstrom G and Ingelman-Sundberg M (1989) Rat liver microsomal NADPH-supported oxidase activity and lipid peroxidation dependent on ethanol-inducible cytochrome P450 (P-450 IIE1) *Biochem Pharmacol* **38:**1313–1318.

Eliasson E, Johansson I, and Ingelman-Sundberg M (1988) Ligand dependent maintenance of ethanol inducible cytochrome P450 in primary rat hepatocyte cultures. *Biochem Biophys Res Commun* **150:**436–443.

Enari M, Talanian RV, Wong WW, and Nagata S (1996) Sequential activation of ICE-like and CPP32-like proteases during *Fas*-mediated apoptosis. *Nature (Lond)* **380:**723–726.

Farber JL (1982) Biology of disease: membrane injury and calcium homeostasis in the pathogenesis of coagulative necrosis. *Lab Invest* **47:**114–123.

Fukuda A, Osawa T, Oda H, Toyokuni S, Satoh K, and Uchida K (1996) Oxidative stress response in iron-induced renal carcinogenesis. *Arch Biochem Biophys* **329:** 39–46.

Goddard JG, and Sweeney GD (1983) Fe-NTA: a potent stimulant of *in vivo* lipid peroxidation in mice. *Biochem Pharmacol* **32:**3879–3882.

Gorsky LD, Koop DR, and Coon MJ (1984) On the stoichiometry of the oxidase and monooxygenase reactions catalyzed by liver microsomal cytochrome P450. *J Biol Chem* **259:**6812–6817.

Halliwell B and Gutteridge JMC (1984) Oxygen toxicity, oxygen radical, transition metals, and disease. *Biochem J* **219:**1–14.

Hawley-Nelson P, Ciccarone V, Gebeyehu G, Jessee J, and Felgner PL (1993) Lipofectamine reagent: a new higher efficiency polycationic liposome transfection reagent. *Focus* **15:**73–79.

Hockenberry DM, Oltvai ZN, Yin XM, Milliman CL, and Korsmeyer SJ (1993) Bcl-2 functions in an antioxidant pathway to prevent apoptosis. *Cell* **75:**241–251.

Kamimura S, Gaal K, Britton RS, Bacon BR, Triadafilopoulos G, and Tsukamoto H (1992) Increased 4-hydroxynonenal levels in experimental alcoholic liver disease: association of lipid peroxidation with liver fibrogenesis. *Hepatology* **16:**448–453.

Krippner A, Matsuno-Yagi A, Gottlieb RA, and Babior BM (1996) Loss of function of cytochrome c in Jurkat cells undergoing *Fas*-mediated apoptosis. *J Biol Chem* **271:**21629–21636.

Kukielka E, Dicker E, and Cederbaum AI (1994) Increased production of reactive oxygen species by rat liver mitochondria after chronic ethanol treatment. *Arch Biochem Biophys* **309:**377–386.

Kurose I, Higuchi H, Miura S, Saito H, Watanabe N, Hokari R, Hirokawa M, Takaishi M, Zeki S, Nakamura T, Ebinuma H, Kato S, and Ishii H (1997) Oxidative stress-mediated apoptosis of hepatocytes exposed to acute ethanol intoxication. *Hepatology* **25:**368–378.

Kyle ME, Nakee D, Sakaida I, Miccadli S, and Farber JL (1988) Endocytosis of SOD is required in order for the enzyme to protect hepatocytes from the cytotoxicity of H_2O_2. *J Biol Chem* **263:**3784–3789.

Lieber CS (1997) Cytochrome P4502E1: its physiological and pathological role. *Physiol Rev* **77:**517–544.

Liu X, Kim CN, Yang J, Jemmerson R, and Wang X (1996) Induction of apoptotic program in cell-free extracts: requirement for dATP and cytochrome c. *Cell* **86:** 147–157.

Martin SJ and Green DR (1995) Protease activation during apoptosis: death by a thousand cuts. *Cell* **82:**349–352.

Merino R, Ding L, Veis DJ, Korsmeyer SJ, and Nunez G (1994) Developmental regulation of the Bcl-2 protein and susceptibility to cell death in β lymphocytes. *EMBO (Eur Mol Biol Organ) J* **13:**683–691.

Morimoto M, Zern MA. Hagbjork AL, Ingelman-Sundberg M, and French SW (1994) Fish oil, alcohol, and liver pathology: role of cytochrome P4502E1. *Proc Soc Exp Biol Med* **207:**197–205.

Mosmann TR (1983) Rapid colorimetric assay for cellular growth and survival: application to proliferation and cytotoxicity assays. *J Immunol Methods* **65:**55–63.

Nordmann R, Ribiere C, and Rouach H (1992) Implications of free radical mechanisms in ethanol-induced cellular injury. *Free Radical Biol Med* **12:**219–240.

Parmley RT, May ME, Spicer SS, Buse MG, and Alvarez CJ (1981) Ultrastructural distribution of inorganic iron in normal and iron-loaded hepatic cells. *Lab Invest* **44:**475–485.

Reed JC (1994) Bcl-2 and the regulation of programmed cell death. *J Cell Biol* **124:**1–6.

Rouach H, Houze P, Orfanilli MT, Gentril M, Bourdon R, and Nordmann R (1990) Effect of acute ethanol administration on the subcellular distribution of iron in rat liver and cerebellum. *Biochem Pharmacol* **39:**1095–1100.

Sadrzzadeh SMH, Nanji AA, and Price PL (1994) The oral iron chelator, 1,2-dimethyl-3-hydroxypyrid-4-one, reduces hepatic-free iron, lipid peroxidation and fat accumulation in chronically ethanol-fed rats. *J Pharmacol Exp Ther* **206:**595–603.

Spach PI and Cunningham CC (1987) Control of state 3 respiration in liver mitochondria from rats subjected to chronic ethanol consumption. *Biochim Biophys Acta* **894:**460–467.

Sturrock A, Alexander J, Lamb J, Craven CM, and Kaplan J (1990) Characterization of a transferrin-independent uptake system for iron in Hela cells. *J Biol Chem* **265:**3139–3145.

Thompson C (1995) Apoptosis in the pathogenesis and treatment of disease. *Science (Washington DC)* **267:**1456–1462.

Tsukamoto H, Horne W, Kamimura S, Niemela O, Parkkaila S, Yla-Hertiuala F, and Brittenham GM (1995) Experimental liver cirrhosis induced by alcohol and iron. *J Clin Invest* **96:**620–630.

Valenzuela A, Fernandez V, and Videla LA (1983) Hepatic and biliary levels of glutathione and lipid peroxides following iron overload in the rat: effect of simultaneous ethanol administration. *Toxicol Appl Pharmacol* **70:**87–95.

Valerio LGX, Parks T, and Peterson DR (1996) Alcohol mediates increases in hepatic serum nonheme iron stores in a rat model for alcohol-induced liver injury. *Alcohol Clin Exp Res* **20:**1352–1361.

Yacoub LK, Fogt F, Griniuviene B, and Nanji AA (1995) Apoptosis and Bcl-2 protein expression in experimental alcoholic liver disease in the rat. *Alcohol Clin Exp Res* **19:**854–859.

Zamzami N, Susin AS, Merchetti P, Hirsch T, Gomez-Monterrey I, Castedo M, and Kroemer G (1996) Mitochondrial control of nuclear apoptosis. *J Exp Med* **183:** 1533–1544.

Zhang H, Loneyl A, and Potter BJ (1993) Effect of chronic alcohol feeding on hepatic iron status and ferritin uptake by rat hepatocytes. *Alcohol Clin Exp Res* **17:**394–400.